AIAA SciTech Forum
23-27 January 2023, National Harbor, MD & Online
AIAA SCITECH 2023 Forum

10.2514/6.2023-2060

Plasma Assisted Emission Control of Hydrocarbon Gas Flares: A 0D Feasibility Study

Praise Noah Johnson*, Taaresh Sanjeev Taneja† and Suo Yang‡
Department of Mechanical Engineering, University of Minnesota – Twin Cities, Minneapolis, MN 55455, USA

Natural gas associated with oil wells and natural gas fields is a significant source of greenhouse gas emissions and airborne pollutants. Flaring of the associated gas removes greenhouse gases like methane and other hydrocarbons. The present study explores the possibility of enhancing the flaring of associated gas mixtures (C_1 – C_4 alkane mixture) using nanosecond pulsed non-equilibrium plasma discharges. Starting with a detailed chemistry for C_0 – C_4 hydrocarbons (Aramco mechanism 3.0 – 589 species), systematic reductions are performed to obtain a smaller reduced mechanism (156 species) yet retaining the relevant kinetics of C_1 – C_4 alkanes at atmospheric pressure and varying equivalence ratios (ϕ = 0.5 – 2.0). This conventional combustion chemistry for small alkanes is then coupled with the plasma kinetics of CH_4, C_2H_6, C_3H_8, and N_2, including electron-impact excitations, dissociations, and ionization reactions. The newly developed plasma-based flare gas chemistry is then utilized to investigate repetitively pulsed non-equilibrium plasma-assisted reforming and subsequent combustion of the flare gas mixture diluted with N_2 at different conditions. The results indicate an enhanced production of hydrogen, ethylene and other species in the reformed gas mixture, owing to the electron-impact dissociation pathways and subsequent H-abstractions and recombination reactions, thereby resulting in a mixture of CH_4, H_2, C_2H_4, C_2H_2, and other unsaturated C_3 species. The reformed mixture shows an enhanced reactivity as exhibited by their shorter ignition delays. The reformed mixture is also observed to undergo increased methane destruction and higher equilibrium temperatures compared to the original mixture as the gas temperature increases, thereby exhibiting a potential for reducing the unburnt emissions of methane and other hydrocarbons.

I. Introduction

Flaring and venting are among the routine daily activities involving the associated gas in petrochemical plants which are uneconomical to extract and are considered safety practices to relieve pressure [1]. The associated gas from petrochemical plants often contains a substantial amount of hydrocarbons and traces of nitrogen and hydrogen sulfide (H_2S) [2]. The hydrocarbons present in these associated gases are primarily C_1-C_4 alkanes such as Methane (CH_4), ethane (C_2H_6), propane (C_3H_8), and butane (nC_4H_{10} and iC_4H_{10}) [2], along with traces of other hydrocarbons. Venting the associated gases into the atmosphere results in a considerable greenhouse effect owing to the 80 times more pronounced greenhouse effect of CH_4 when compared to CO_2 [3–5]. Therefore, it is necessary to flare the associated gas, thereby releasing CO_2 and H_2O into the atmosphere instead of strong greenhouse gases like CH_4. Regardless, studies [6, 7] observed flares operating outside stable operating conditions to result in unstable flares, thereby causing a reduction in combustion and CH_4 destruction efficiencies. Thus, unstable flaring can result in a significant greenhouse effect and affect air quality standards due to CH_4 emissions and black carbon arising from the incomplete combustion of associate gases [2]. Consequently, it is paramount to explore better flaring techniques for promoting the complete flaring of the associate gases.

In order to facilitate complete flaring and improve methane destruction efficiency (> 99.5% destruction or removal efficiency of methane) of an associated gas largely composed of C_1 – C_4 alkanes, it is necessary to improve the reactivity (increased adiabatic flame temperature (T_{ad}), ignition delays, flame speeds) of the gas mixture. The reformed mixture can then undergo a complete flaring process on account of the increased reactivity of the associated gas mixture. One way to enhance the reactivity of the gas mixture is to perform a plasma-assisted fuel reforming, where, the gas mixture can be reformed to a more reactive mixture by the application of nanosecond pulsed non-equilibrium plasma discharges [8, 9]. The application of nanosecond non-equilibrium plasma to associated gas mixtures can result in

*Ph.D. Student, Student Member AIAA
†Ph.D. Candidate, Student Member AIAA.
‡Richard & Barbara Nelson Assistant Professor, suo-yang@umn.edu (Corresponding Author), Senior Member AIAA.

the production of electrons, excited, and charged species [10, 11]. In addition, plasma-assisted reforming (PAR) give rise to several reactive radicals such as H and CH_3 due to the proceeding of electron impact dissociation reactions involving CH_4 ($e^- + CH_4 \longrightarrow e^- + CH_x + (_4-x)H$). These reactions, along with the subsequent H-abstractions and recombinations results in the production of H_2 and other alkene species. The enhanced reactivity of the reformed gas mixture can be attributed to the production of reactive species such as H_2 (T_{ad} = 2483 K), ethylene (C_2H_4 : T_{ad} = 2375 K), and acetylene (C_2H_2 : T_{ad} = 2773 K) in the CH_4-dominant gas mixture (T_{ad} = 2236 K) [12]. Thus, it is imperative to investigate the viability of plasma-assisted systems in flare gas reforming and the role of fuel reforming in controlling flare emissions.

The present study probes into the feasibility and kinetics of non-equilibrium repetitive pulsed plasma-assisted fuel reforming of flare gases to control flare emissions. A plasma-assisted fuel reforming mechanism for the flare gases will be developed and used to investigate the effect of fuel reforming in the production of reactive species. The impact of different classes of plasma reactions on fuel reforming will be analyzed using a plasma-based Global Pathway Anaylyis (PGPA) algorithm [13]. This article is organized as follows. Section II discusses the methodology and considerations involved in the numerical simulations of plasma-assisted fuel reforming, along with the kinetics of plasma assisted flare gas reforming. The numerical results of flare gas reforming and its effect on flaring emissions and mixture reactivity are presented in Sec. III, following which, the conclusions are summarized in Sec. IV.

II. Methodology

A. Numerical methodology

An in-house zero-dimensional (0D) code [14, 15] for a homogeneous isobaric reactor is used to model the nanosecond, repetitive pulsed non-equilibrium plasma discharges into the gas mixture. The plasma kinetics is handled by a 0D plasma kinetics code ZDPlasKin [16], whereas the combustion chemistry is solved using CHEMKIN-III [17] subroutines. A detailed description of the solver can be found elsewhere in the literature [14, 18, 19]. In the present study, simulations are performed considering a reduced electric fields (E/N) of 100 and 300 Td (1 Td = 10^{-17} V cm^2) and energy deposition per pulse of 0.05 J/cm^3, to achieve convergence. The maximum pulse duration is limited to 20 nanoseconds. Considering a very short flow residence time in practical flare systems, the simulations are done at a high pulsing frequency of 100 kHz and the total number of pulsed discharges is fixed to 30 pulses, to maintain the conditions necessary for a diffuse discharge [20]. The calculations are performed for an inlet gas temperature of 300 K and pressure of 1 atm.

B. Plasma kinetics

The plasma kinetics governs the chemistry of plasma-assisted reforming (PAR) of the flare gases. Plasma discharges, resulting in the production of charged particles (electrons and ions) and various excited species, catalyze the production of radicals in the system, thereby enhancing the reactivity and heat release [21]. In PAR systems, these electrons and excited species aid in the decomposition of gas components to smaller radicals, promoting the formation of a reformed reactive gas mixture [22, 23]. The plasma chemistry involves many new reaction classes such as electron impact ionization, excitation, dissociative excitation, dissociative ionization, dissociation, de-excitation, attachment, and recombination reactions [21]. These new classes of reactions governing the plasma kinetics can be coupled with conventional combustion kinetics to construct the detailed PAR and oxidation chemistry [21, 23]. The inclusion of plasma reactions, whose rates depend on the reduced electric field (E/N) and cross sections of the colliding species, introduce additional complexity to the previously intricate combustion kinetics. Adding to the challenges, often, there exist a dearth in the availability of detailed plasma chemistry, even for the simplest of hydrocarbons.

The present study considers the electron-impact reactions of four major species (CH_4, C_2H_6, C_3H_8, and N_2) The electron-impact reactions of the aforementioned species are obtained from different LxCAT online databases [24–27]. The N_2 chemistry consist of electron impact excitation (vibrational and electronic), dissociation, and ionization of N_2. Eight vibrational modes ($N_2(v_1 - v_8)$) and four electronic modes (N_2(A), N_2(B), N_2(a′), and N_2(C)) are considered for N_2 excitation [15]. The plasma chemistry for the CH_4 sub mechanism is obtained from Mao et al. [19]. The mechanism contains electron impact excitation (vibrational), dissociation, and ionization. Two vibrational modes ($CH_4(v_{24})$ and $CH_4(v_{13})$) are considered in this study. For the C_2H_6 and C_3H_8 sub-mechanism, two vibrational states each ($C_2H_6(v_{24})$ and $C_2H_6(v_{13})$ for C_2H_6, and $C_3H_8(v_1)$ and $C_3H_8(v_2)$ for C_3H_8) are considered. In addition to these reactions, the reactions among H_2, CH_4, and various C_2 and C_3 species and intermediates with the excited states of N_2 and other radical species are also considered for completeness from the literature [28] in the present work. Finally, the current

Table 1 Different ground state species and the corresponding excited and charged species considered in the current study

Ground state	Excited states	Charged derivatives
N_2	$N_2(v_1)$, $N_2(v_2)$, $N_2(v_3)$, $N_2(v_4)$ $N_2(v_5)$, $N_2(v_6)$, $N_2(v_7)$, $N_2(v_8)$ $N_2(A)$, $N_2(B)$, $N_2(a')$, $N_2(C)$, $N(_2P)$, $N(_2D)$	N^+, N_2^+, N_3^+, N_4^+
H_2	–	H^+, H_2^+, H_3^+
CH_4	$CH_4(v_{24})$, $CH_4(v_{13})$	C^+, CH^+, CH_2^+, CH_3^+, CH_4^+
C_2H_6	$C_2H_6(v_{24})$, $C_2H_6(v_{13})$	C_2H^+, $C_2H_2^+$, $C_2H_3^+$, $C_2H_4^+$, $C_2H_5^+$, $C_2H_6^+$, $C_2H_7^+$
C_3H_8	$C_3H_8(v_1)$, $C_3H_8(v_2)$	$H_2C_3H^+$, $C_3H_3^+$, $C_3H_4^+$, $C_3H_5^+$, $C_3H_6^+$, $C_3H_7^+$, $C_3H_8^+$, $C_4H_2^+$, $C_4H_3^+$, $C_4H_5^+$

study considers electronic excitation of C_1 – C_4 alkanes and the subsequent dissocaition of excited electronic state as a single lumped reaction assuming ultra fast dissociation of the excited state. Table 1 lists the ground state species and the corresponding excited and charged species considered in the present work.

C. Combustion kinetics

The reformed gas mixture is anticipated to contain H_2, C_2H_2, C_2H_4, C_3H_6, and C_3H_4, in addition to the original components of the flare gas. Thus, in order to simulate the flaring of the reformed gas mixture, it is vital to incorporate the oxidation kinetics of the aforementioned components in the kinetic model. To achieve this, a comprehensive model (Aramco mechanism 3.0) for the oxidation of C_0-C_4 [29] is chosen as the reference combustion kinetic mechanism for small alkane oxidation. The Aramco mechanism is a detailed mechanism with 581 species 3037 reactions and has been extensively validated for the kinetics of H_2, CH_4, various C_1 and C_2 components, propene (C_3H_6), allene (C_3H_4-A), propyne (C_3H_4-P), dimethyl ether (CH_3OCH_3), isobutene (i-C_4H_8), 1- and 2-butene (C_4H_8-1 and C_4H_8-2), and 1,3-butadiene (C_4H_6). Nevertheless, the original Aramco mechanism is complex and the large number of species and accompanying reactions presents a formidable challenge in numerical simulations. Thus, it is necessary to reduce the detailed Aramco mechanism to obtain a reduced Aramco model for the flare chemistry.

A global pathway selection-based reduction algorithm (GPS) [30] is chosen as the reduction methodology to reduce the detailed Aramco mechanism. Ten different fuels (H_2, CH_4, C_2H_2, C_2H_4, C_2H_6, C_3H_4-A, C_3H_4-P, C_3H_6, C_3H_8, and C_4H_{10}) are chosen as the reduction target fuels whose essential chemistry is sought to be retained. The reduction is carried out considering a reference simulation dataset of 0D isobaric ignition delays at different pressures (0.1, 1.0, and 10 atm), temperatures (800-1800 K), and equivalence ratios (0.5-2.0) so as to retain the relevant combustion chemistry at the aforementioned thermodynamic conditions. Among different reduced versions, a reduced mechanism consisting of 156 species and 1069 reactions is chosen as the flare combustion chemistry. This reduced Aramco mechanism is then validated against the simulation dataset of the detailed Aramco mechanism to establish the chemical accuracy and consistency of the reduced mechanism.

Figure 1 shows the comparison of ignition delay times between the detailed and reduced Aramco mechanism at 1 atm for target component fuels (CH_4 and C_2H_6) and at different equivalence ratios. A very good agreement between the detailed and reduced mechanism (within 5% reduction tolerance) is observed between the reduced and detailed

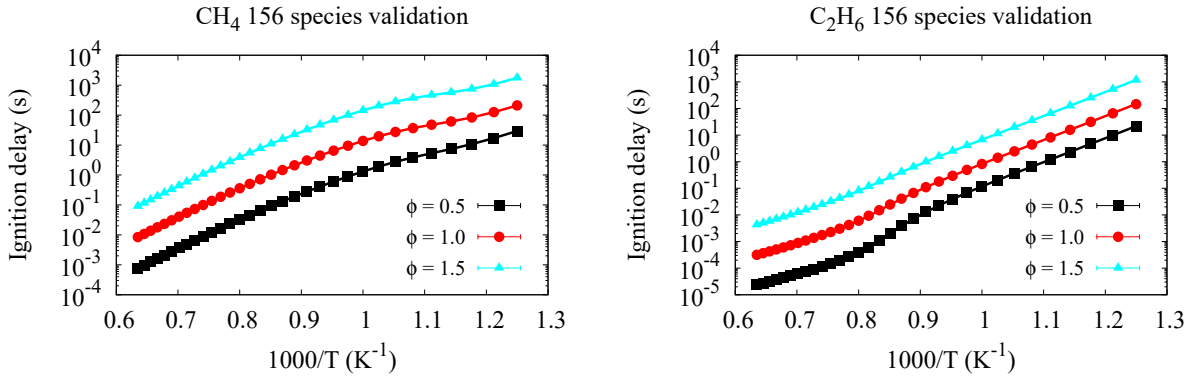

(a) CH_4 (b) C_2H_6

Fig. 1 Comparison ignition delays for the target fuels (CH_4 and C_2H_6) between the detailed and reduced mechanism at 1 atm. The symbols correspond to the simulated results using the detailed Aramco mechanism [29] and the lines represent simulated results using the reduced Aramco mechanism. The results for ϕ = 1.0 and 1.5 are multiplied by 10 and 100 respecrively for clarity.

mechanism. Any further reduction was observed to reduce the accuracy of reduced mechanism, thereby resulting in an error greater than 5%. Thus, the reduced Aramco mechanism at 156 species and 1069 reactions is considered as the chemical kinetic mechanism for the oxidation of reformed flare gas. The flare combustion model derived from the Aramco mechanism is then systematically appended with the plasma kinetic model from the present work to obtain a coupled plasma-assisted reforming and combustion mechanism for flare gas reforming and oxidation.

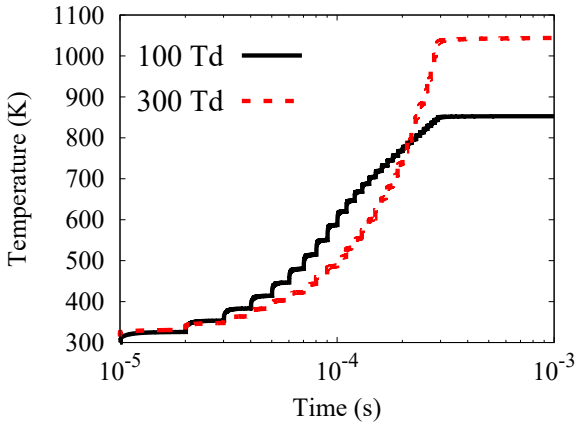

Fig. 2 Evolution of temperature for the plasma-assisted reforming of flare fas-N_2 mixture at a.) E/N = 100 Td (solid black line) and b.) E/N = 300 Td (dashed red line) using non-equilibrium plasma discharges in a 0D isobaric reactor.

III. Results and Discussion

This section presents the numerical results of the plasma-assisted reforming of flare gas/N_2 mixture (ratio of 0.6:0.4) and the impact of fuel reforming on the methane destruction and reactivity of flare gas. The flare gas considered in the present study is a mixture of CH_4, C_2H_6, C_3H_8, and C_4H_{10} in a concentration ratio of 0.65:0.2:0.1:0.05. Two different reduced electric fields (E/N) are utilized in calculations to understand the effect of different modes of excitations (electronic and vibrational) on gas reforming.

A. Plasma-assisted reforming at different E/N

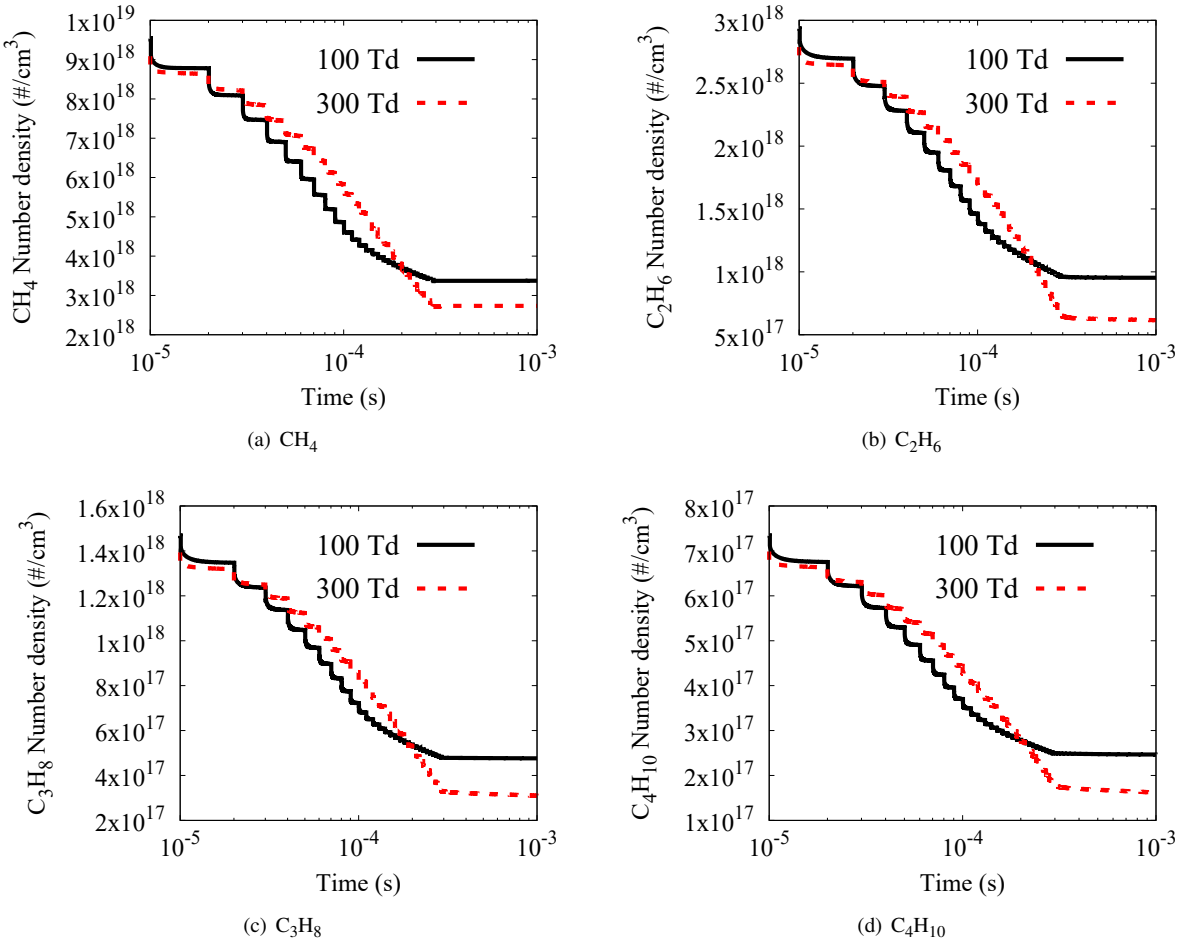

(a) CH_4 (b) C_2H_6 (c) C_3H_8 (d) C_4H_{10}

Fig. 3 Evolution of species number densities of flare gas components during plasma-assisted reforming of the mixture at E/N = 100 Td (solid black line) and 300 Td (dashed red line) using non-equilibrium plasma discharges in a 0D isobaric reactor.

To understand the effect of plasma in producing reactive species and enhancing the reactivity of the associated gas, simulations are performed for nanosecond pulsed non-equilibrium plasma discharge in the flare gas mixture diluted by N_2 (40% dilution) at two different reduced electric fields (E/N = 100 and 300 Td). Fig. 2 depicts the evolution of temperature during the nanosecond pulses. At the end of plasma discharges, the mixture at 300 Td is found to achieve a higher reformed gas temperature (~1050 K) when compared to reforming at 100 Td (~850 K). This higher temperature at 300 Td can be attributed to the activation of electronic excitations and associated dissociations of different alkane species (ultra-fast heating and radical production) as compared to the vibrational excitations at 100 Td.

In addition to the rise in temperature, the number densities of the flare gas components are observed to reduce dueing plasma discharges. Figure 3 shows the evolution of number densities of the different flare gas species undergoing plasma reforming. It can be observed that the number density of CH_4 (Fig. 3 (a)) falls from $\sim 1 \times 10^{19}$ to $\sim 3 \times 10^{18}$ (about 70% drop) at the end of plasma discharge (3×10^{-4} s). This drop represents the reduction in available quantity of CH_4 species before flaring, which can significantly reduce the amount of unburnt CH_4 emissions. Moreover, the increased temperatures equate to an increased reactivity of the gas mixture, thereby promoting fuel cracking, reducing the amount of available CH_4 in the gas mixture before flaring. Figure 3 (b, c, and d) also portrays the evolution of C_2H_6, C_3H_8, and C_4H_{10}, where, a similar phenomena is observed. Despite the flare gas being reformed at both 100 and 300 Td, the latter case if found to impart a higher level of flare gas reduction (30-60% more drop in number densities) compared to the former.

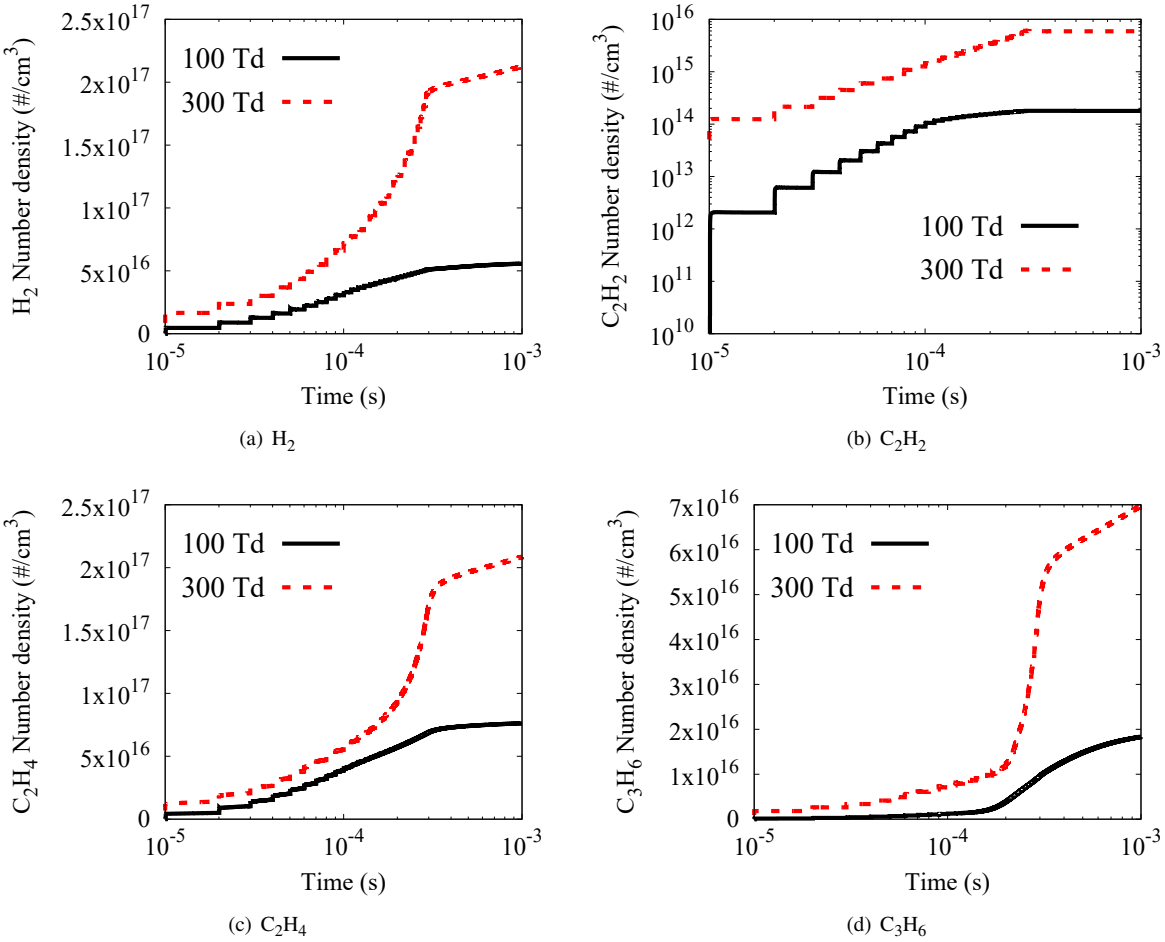

Fig. 4 Evolution of species number densities of other reactive species (H_2, C_2H_2, C_2H_4, and C_3H_6) during plasma-assisted reforming of the mixture at E/N = 100 Td (solid black line) and 300 Td (dashed red line) using non-equilibrium plasma discharges in a 0D isobaric reactor.

Figure 4 shows the production of different reactive species effected by plasma discharges at both 100 and 300 Td. From Fig. 4 (a), it can be observed that at 300 Td, H_2 number densities are significantly higher (~4x) compared to that at 100 Td. Similar observations are made for other reactive species (see Fig. 4 (b, c, and d)) C_2H_2 (~10x), C_2H_4 (~2x), and C_3H_6 (~4x). The presence of H_2 in the associated gas mixture will result in reduced emissions of hydrocarbons such as aldehydes (CH_2O and CH_3CHO) and also lowers the production of soot due to the prominence of low carbon reaction pathways facilitated by H_2 [31]. Besides, the presence of H_2, C_2H_4, and other reactive species can result in increased adiabatic flame temperatures and laminar flame speeds of the gas mixture [31, 32], which can affect to improve the reactivity and reduce the flare emissions due to unburnt gases. Thus reforming at higher reduced electric fields (E/N = 300 Td), is observed to impart a improved level of reforming and higher gas temperatures.

B. Global pathway analysis of plasma-assisted reforming

To understand the increased reforming at higher E/N, a plasma-based global pathway analysis (PGPA) [13] is performed to identify the reforming channels during the plasma pulse. Table 2 shows the major reforming pathways and prominent excitation and de-excitation channels (cycles) for the production of variuos reactive species (H_2, C_2H_2, C_2H_4, and C_3H_6) at 100 Td. The global pathways and cycles are identified based on the quantification of radical production rates (of H, CH_3, etc.) produced through the respective pathway/cycle. From Table 2, it can be observed that the pathway $CH_4 \longrightarrow CH_4^+ \longrightarrow C_2H_4^+ \longrightarrow C_2H_5^+ \longrightarrow C_2H_6 \longrightarrow CH_3 \longrightarrow C_3H_8 \longrightarrow C_2H_5 \longrightarrow C_2H_4$ results

Table 2 Global pathways and cycles governing the production of reformed mixture based on radical production rate for the nanosecond discharge plasma reforming of flare gas mixture at 100 Td.

Reformed species	Global pathways/cycles	Radical production rate (mol/cm^{3}s)
H_2	$CH_4 \longrightarrow CH_3 \longrightarrow C_3H_8 \longrightarrow C_2H_5 \longrightarrow C_2H_4 \longrightarrow C_2H_5^+ \longrightarrow C_2H_6 \longrightarrow H_2$	0.00034
	$C_2H_6 \longrightarrow CH_3 \longrightarrow C_2H_5 \longrightarrow C_2H_4 \longrightarrow H_2$	0.00045
	$C_3H_8 \longrightarrow C_2H_5 \longrightarrow C_2H_4 \longrightarrow C_2H_4^+ \longrightarrow C_2H_5^+ \longrightarrow C_2H_6 \longrightarrow H_2$	0.00021
C_2H_2	$CH_4 \longrightarrow CH_4^+ \longrightarrow C_2H_5^+ \longrightarrow C_2H_6 \longrightarrow CH_3 \longrightarrow C_3H_8 \longrightarrow C_2H_5 \longrightarrow C_2H_4 \longrightarrow C_2H_2$	0.00077
	$C_2H_6 \longrightarrow CH_3 \longrightarrow C_3H_8 \longrightarrow C_2H_5 \longrightarrow C_2H_4 \longrightarrow C_2H_2$	0.00077
	$C_3H_8 \longrightarrow C_2H_5 \longrightarrow C_2H_4 \longrightarrow C_2H_4^+ \longrightarrow C_2H_5^+ \longrightarrow C_2H_6 \longrightarrow H_2$	0.00021
C_2H_4	$CH_4 \longrightarrow CH_4^+ \longrightarrow C_2H_4^+ \longrightarrow C_2H_5^+ \longrightarrow C_2H_6 \longrightarrow CH_3 \longrightarrow C_3H_8 \longrightarrow C_2H_5 \longrightarrow C_2H_4$	0.00096
	$C_2H_6 \longrightarrow CH_3 \longrightarrow C_3H_8 \longrightarrow C_2H_5 \longrightarrow C_2H_4$	0.00087
	$C_3H_8 \longrightarrow C_2H_5 \longrightarrow CH_4 \longrightarrow CH_4^+ \longrightarrow C_2H_4^+ \longrightarrow C_2H_5^+ \longrightarrow C_2H_6 \longrightarrow CH_3 \longrightarrow C_2H_4$	0.00043
C_3H_6	$CH_4 \longrightarrow CH_4^+ \longrightarrow C_2H_5^+ \longrightarrow C_2H_6 \longrightarrow CH_3 \longrightarrow C_2H_4 \longrightarrow C_2H_4^+ \longrightarrow C_2H_5 \longrightarrow C_3H_8 \longrightarrow C_3H_7{-}I \longrightarrow C_3H_6$	0.00081
	$C_2H_6 \longrightarrow C_2H_5 \longrightarrow C_2H_4 \longrightarrow C_2H_4^+ \longrightarrow C_3H_7^+ \longrightarrow C_3H_5{-}A \longrightarrow CH_4 \longrightarrow CH_3 \longrightarrow C_3H_8 \longrightarrow C_3H_7{-}I \longrightarrow C_3H_6$	0.00029
	$C_3H_8 \longrightarrow C_2H_5 \longrightarrow C_2H_4 \longrightarrow C_2H_3 \longrightarrow C_3H_6$	0.00041
	Cycles assisting reforming	
	$N_2 \longrightarrow N_2(B) \longrightarrow N_2(A) \longrightarrow N_2$	0.00083
	$N_2 \longrightarrow N_2(B) \longrightarrow N_2$	0.00028
	$N_2 \longrightarrow N_2(A) \longrightarrow N_2$	0.00027

in the highest radical radical production of ~0.001 mol/cm^{3}s. Moreover, the cycles assisting reforming and radical production involve the electronic excited states of N_2 ($N_2 \longrightarrow N_2(B) \longrightarrow N_2(A) \longrightarrow N_2$) with a maximum radical production rate of ~0.0008 mol/cm^{3}s. However, at 300 Td (see Table 3), global pathways and cycles for the production of reformed species exhibit significantly boosted radical production rates (3 orders of mignitute higher). The major radical producing cycle at 300 Td is found to be $N_2 \longrightarrow N_2(C) \longrightarrow N_2$ (~ 0.1 mol/cm^{3}s), an electronic excitation-deexcitation cycle as was the case for 100 Td. Nevertheless, the higher reduced electric field contributes a significant portion of the deposited plasma energy to electronic mode as compared to 100 Td, thereby elevating the radical production at 300 Td.

Similar to cycles, the first step of global pathways often involve an electron-impact reaction to produce a radical (CH_3, C_2H_5, etc.) or charged species (CH_3^+, CH_4^+, $C_2H_5^+$, etc.). These rates of such electron impact reactions significantly depend on E/N and deposited plasma energy. As E/N is increased to 300 Td, the prominence of these electron impact dissociation (e.g. $E + CH_4 \longrightarrow E + CH_3 + H$) and ionization reaction ($E + CH_4 \longrightarrow {}_2E + CH_4^+$) increases, resulting in improved reforming. This is evident from global pathways depicting orders of magnitude higher radical production rates (highest being 0.46 mol/cm^{3}s through $C_2H_6 \longrightarrow CH_3 \longrightarrow CH_3^+ \longrightarrow CH_4^+ \longrightarrow C_2H_4^+ \longrightarrow C_3H_7^+ \longrightarrow C_3H_5{-}A \longrightarrow C_3H_6$) compared to 100 Td. In addition, the contribution of charged species in global pathways are found to increase at higher E/N, bolstering the ability to produce further radicals. Once the radical pool and charged species are generated, the production of reformed species (H_2, C_2H_4) are found to be effected by subsequent H-abstractions (e.g. $C_2H_5 \longrightarrow C_2H_4$, $C_2H_4^+ \longrightarrow C_2H_2$) and radical-radical recombinations ()e.g. $H \longrightarrow$

Table 3 Global pathways and cycles governing the production of reformed mixture based on radical production rate for the nanosecond discharge plasma reforming of flare gas mixture at 300 Td.

Reformed species	Global pathways/cycles	Radical production rate (mol/cm^{3}s)
H_2	$CH_4 \longrightarrow CH_3^+ \longrightarrow CH_4^+ \longrightarrow C_2H_4^+ \longrightarrow C_2H_5^+ \longrightarrow C_2H_6 \longrightarrow CH_3 \longrightarrow CH_2^+ \longrightarrow H_2$	0.31
	$C_2H_6 \longrightarrow CH_3 \longrightarrow CH_3^+ \longrightarrow CH_4^+ \longrightarrow CH_4 \longrightarrow H \longrightarrow H_2$	0.31
	$C_3H_8 \longrightarrow C_2H_5 \longrightarrow C_2H_4 \longrightarrow C_2H_5^+ \longrightarrow C_2H_6 \longrightarrow CH_3 \longrightarrow CH_2^+ \longrightarrow H_2$	0.2
C_2H_2	$CH_4 \longrightarrow CH_4^+ \longrightarrow C_2H_5^+ \longrightarrow C_2H_6 \longrightarrow CH_3 \longrightarrow CH_2^+ \longrightarrow C_2H_4^+ \longrightarrow C_2H_5 \longrightarrow C_2H_4 \longrightarrow C_2H_2$	0.28
	$C_2H_6 \longrightarrow CH_3 \longrightarrow CH_3^+ \longrightarrow CH_4^+ \longrightarrow C_2H_4^+ \longrightarrow C_2H_2$	0.34
	$C_3H_8 \longrightarrow C_2H_5 \longrightarrow C_2H_4 \longrightarrow C_2H_6 \longrightarrow CH_3 \longrightarrow CH_3^+ \longrightarrow CH_4^+ \longrightarrow C_2H_4^+ \longrightarrow C_2H_2$	0.27
C_2H_4	$CH_4 \longrightarrow CH_4^+ \longrightarrow C_2H_4^+ \longrightarrow C_2H_5^+ \longrightarrow C_2H_6 \longrightarrow CH_3 \longrightarrow C_3H_8 \longrightarrow C_2H_5 \longrightarrow C_2H_4$	0.36
	$C_2H_6 \longrightarrow CH_3 \longrightarrow CH_3^+ \longrightarrow CH_4^+ \longrightarrow C_2H_4^+ \longrightarrow C_2H_5 \longrightarrow C_2H_4$	0.44
	$C_3H_8 \longrightarrow C_2H_5 \longrightarrow CH_4 \longrightarrow CH_3 \longrightarrow CH_3^+ \longrightarrow CH_4^+ \longrightarrow C_2H_4^+ \longrightarrow C_2H_5^+ \longrightarrow C_2H_6 \longrightarrow C_2H_4$	0.13
C_3H_6	$CH_4 \longrightarrow CH_4^+ \longrightarrow C_2H_5^+ \longrightarrow C_2H_6 \longrightarrow CH_3 \longrightarrow CH_2^+ \longrightarrow C_2H_4^+ \longrightarrow C_2H_5 \longrightarrow C_3H_8 \longrightarrow C_3H_8^+ \longrightarrow C_3H_6$	0.3
	$C_2H_6 \longrightarrow CH_3 \longrightarrow CH_3^+ \longrightarrow CH_4^+ \longrightarrow C_2H_4^+ \longrightarrow C_3H_7^+ \longrightarrow C_3H_5{-}A \longrightarrow C_3H_6$	0.46
	$C_3H_8 \longrightarrow C_2H_5 \longrightarrow C_2H_4 \longrightarrow C_2H_6 \longrightarrow CH_3 \longrightarrow CH_3^+ \longrightarrow CH_4^+ \longrightarrow C_2H_4^+ \longrightarrow C_3H_7^+ \longrightarrow C_3H_5{-}A \longrightarrow C_3H_6$	0.35
	Cycles assisting reforming	
	$N_2 \longrightarrow N_2(B) \longrightarrow N_2(A) \longrightarrow N_2$	0.018
	$N_2 \longrightarrow N_2(B) \longrightarrow N_2$	0.024
	$N_2 \longrightarrow N_2(C) \longrightarrow N_2$	0.1

H_2, $C_3H_5{-}A \longrightarrow C_3H_6$).

In addition to the improved number densities of reformed species (see Fig. 4), a higher gas temperature was also observed to be effected at 300 Td (see Fig. 2). To delineate the higher heating at 300 Td, it is necessary to investigate the gas heating imparted by various pathways and cycles. Table 4 portrays the global pathways and cycles governing the gas heating of the flare gas mixture at 100 and 300 Td. At 100 Td, the major gas heating cycle is observed to be $N_2 \longrightarrow N_2(B) \longrightarrow N_2(A) \longrightarrow N_2$ (841 W/cm^3). The next cycle involves the vibrational cascade of N_2 ($N_2 \longrightarrow N_2(v_8) \longrightarrow N_2(v_7) \longrightarrow N_2(v_6) \longrightarrow N_2(v_5) \longrightarrow N_2(v_4) \longrightarrow N_2(v_3) \longrightarrow N_2(v_2) \longrightarrow N_2(v_1) \longrightarrow N_2$), imparting a gas heating of 615 W/cm^3. Similar values of heating are found to be bestowed by global pathways ($C_2H_6 \longrightarrow C_2H_4 \longrightarrow C_2H_3 \longrightarrow C_3H_6$, 239 W/cm^3) at 100 Td. However, as E/N is increased to 300 Td, the electronic excitation cycles of N_2 alone plays the major role in gas heating, with $N_2 \longrightarrow N_2(a') \longrightarrow N_2$ (150,436 W/cm^3) releasing about three orders of magnitude large heat release as compared to 100 Td. Similarly high numbers can also be observed with other cycles and global pathways at 300 Td. This significantly high heat release is a consequence of more energy being distributed to electronic mode compared to vibrational modes. In addition, the improved radical production at 300 Td can result in the activation of additional heat release reactions, which would not be possible in the absence of high E/N plasma discharges.

Table 4 Major heat releasing cycles and global pathways governing the production of reformed mixture by nanosecond discharge plasma at 100 and 300 Td.

Reduced electric field (Td)	Global pathways/cycles	Heat release (W/cm^3)
100	*Cycles*	
	$N_2 \longrightarrow N_2(B) \longrightarrow N_2(A) \longrightarrow N_2$	841
	$N_2 \longrightarrow N_2(v_8) \longrightarrow N_2(v_7) \longrightarrow N_2(v_6) \longrightarrow N_2(v_5) \longrightarrow N_2(v_4) \longrightarrow N_2(v_3) \longrightarrow N_2(v_2) \longrightarrow N_2(v_1) \longrightarrow N_2$	615
	$C_2H_6 \longrightarrow C_2H_6(v_{13}) \longrightarrow C_2H_6(v_{24}) \longrightarrow C_2H_6$	108
	Global pathways	
	$CH_4 \longrightarrow CH_3 \longrightarrow C_2H_6 \longrightarrow C_2H_4 \longrightarrow C_2H_4^+ \longrightarrow C_3H_7^+ \longrightarrow C_3H_5{-}A \longrightarrow C_3H_6$	266
	$C_2H_6 \longrightarrow C_2H_4 \longrightarrow C_2H_3 \longrightarrow C_3H_6$	239
	$CH_4 \longrightarrow CH_4^+ \longrightarrow C_2H_4^+ \longrightarrow C_2H_5 \longrightarrow C_3H_8 \longrightarrow C_3H_7{-}I \longrightarrow C_3H_6 \longrightarrow CH_3 \longrightarrow C_2H_6 \longrightarrow C_2H_4$	210
	$CH_4 \longrightarrow CH_4^+ \longrightarrow C_2H_4^+ \longrightarrow C_2H_5 \longrightarrow C_3H_8 \longrightarrow C_3H_7{-}I \longrightarrow C_3H_6 \longrightarrow CH_3 \longrightarrow C_2H_6 \longrightarrow C_2H_4 \longrightarrow C_2H_2$	204
300	*Cycles*	
	$N_2 \longrightarrow N_2(a') \longrightarrow N_2$	150436
	$N_2 \longrightarrow N_2(C) \longrightarrow N_2(a') \longrightarrow N_2$	53770
	$N_2 \longrightarrow N_2(C) \longrightarrow N_2$	44305
	$N_2 \longrightarrow N_2(B) \longrightarrow N_2(A) \longrightarrow N_2$	20816
	Global pathways	
	$CH_4 \longrightarrow CH_3 \longrightarrow CH_3^+ \longrightarrow CH_4^+ \longrightarrow C_2H_5^+ \longrightarrow C_2H_6 \longrightarrow C_2H_4 \longrightarrow C_2H_4^+ \longrightarrow C_3H_7^+ \longrightarrow C_3H_5{-}A \longrightarrow C_3H_6$	73007
	$CH_4 \longrightarrow CH_3 \longrightarrow CH_3^+ \longrightarrow CH_4^+ \longrightarrow C_2H_4^+ \longrightarrow C_2H_5^+ \longrightarrow C_2H_6 \longrightarrow C_2H_4$	70602
	$CH_4 \longrightarrow CH_3 \longrightarrow CH_3^+ \longrightarrow CH_4^+ \longrightarrow C_2H_4^+ \longrightarrow C_2H_5^+ \longrightarrow C_2H_6 \longrightarrow C_2H_4 \longrightarrow C_2H_2$	60170
	$C_2H_6 \longrightarrow C_2H_4 \longrightarrow C_2H_4^+ \longrightarrow C_3H_7^+ \longrightarrow C_3H_5{-}A \longrightarrow C_3H_6$	48545

C. Effect of plasma-assisted reforming on reactivity

To perceive the importance of plasma-assisted fuel reforming in improving the reactivity of flare gas mixtures, 0D homogeneous isobaric ignition delay simulations are performed at ϕ = 1.5 and atmospheric pressures for the original flare gas and reformed mixtures at 100 and 300 Td (see Fig. 5). At the lowest temperature (800 K), the flare gas mixture ignites at about 8.2 seconds, while the reformed gas mixtures at 300 and 100 Td are observed to ignite much faster (5 and 6.2 seconds respectively). This amounts to 24% and 40% faster ignition delays, a significant improvement to the reactivity at low temperatures [33], thereby, suggesting the significance of plasma reforming in aiding the flaring at low temperature scenarios (heat loss during winter). Overall at different gas temperatures, the reformed gas mixture exhibits improved reactivity in an order 300 Td > 100 Td > Original gas.

Figure 6 shows the variation of adiabatic flame temperatures and equilibrium mole fractions of CH_4 at different initial mixture temperatures for the reformed (300 Td) and original flare gas mixtures. From Fig. 6 (a), it can be observed that reformed gas mixture exhibits an overall improved flame temperatures (10-20 K higher) compared to original mixture. The reformed mixture is also shown to exhibit reduced equilibrium CH_4 levels (5-10% reduction) compared to the flare gas (see Fig. 6 (b)). Further increase inadiabatic flame temperatures and CH_4 destruction can be achieved by either increasing the plasma energy deposition or reduced electric field, thereby activating new electronic modes of excitations and dissociation reactions to aid in reforming the gas mixture.

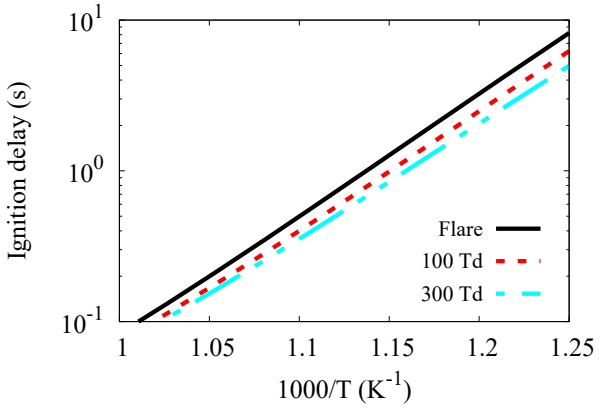

Fig. 5 Comparison of ignition delay times of the reformed (dotted lines) and original flare gas mixture (solid line) at ϕ = 1.5 in a homogeneous batch reactor.

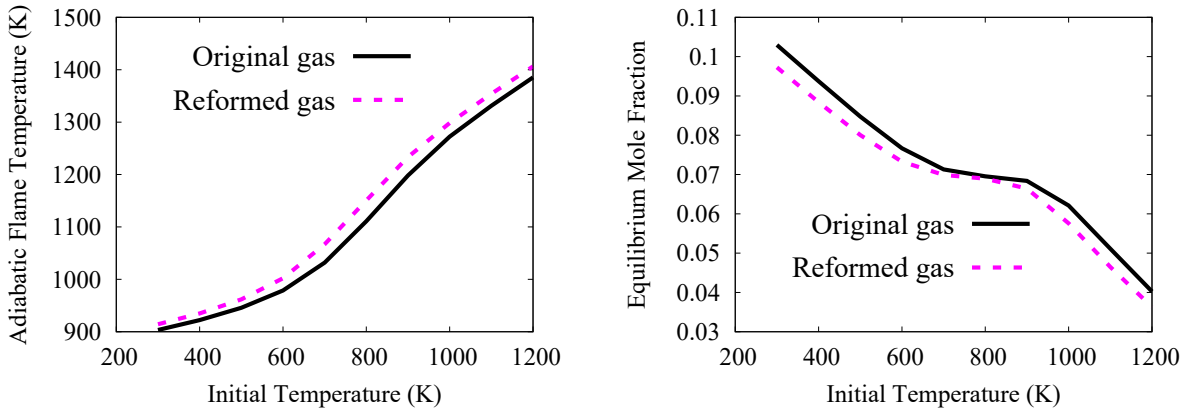

(a) Adiabatic flame temperatures

(b) Equilibrium CH_4 concentrations

Fig. 6 Variation of a.) adiabatic flame temperatures and b.) equilibrium mole fractions of CH_4 at different initial mixture temperatures for the reformed (dashed magenta lines) and original flare gas (solid black lines) mixtures.

To summarize, plasma-assisted flare gas reforming is found to promote gas reactivity and improved levels of CH_4 destruction at low temperatures, owing to the activation of electronic states and their reactions. Further improvements in reactivity and CH_4 destruction is possible by simply operating the plasma reforming at higher discharge voltages and smaller gap distance between electrodes, facilitating a higher reduced electric field.

IV. Conclusion and Future Work

The plasma-assisted fuel reforming of associated gas mixtures (CH_4/C_2H_6/C_3H_8/C_4H_{10}/diluent) has been numerically probed into using an in-house 0D code for nanosecond pulsed non-equilibrium plasma discharges. A detailed combustion chemistry for smaller alkanes (Aramco Mechanism 3.0) has been systematically reduced and coupled with the plasma chemistry of different alkanes and N_2 from the literature. The coupled plasma-assisted reforming and combustion mechanism was used to simulate fuel reforming of flare gas/N_2 mixture affected by nanosecond pulsed non-equilibrium plasma discharges. The results showed appreciable production of reactive fuels such as H_2, C_2H_2, and C_2H_4, in addition to the increased temperature of the gas mixture. Reforming at a higher reduced electric field was found to promote improved reforming, mixture reactivity, and increased CH_4 destruction when compared to reforming at a lower reduced electric field. In particular, the reformed mixture exhibited improved reactivity at low temperature conditions, asserting

the usefulness of plasma-assisted fuel reforming for reactivity at colder conditions.

The present work is the foremost in investigating the ability of plasma reforming in improving flare gas reactivity and subsequent emission control at adverse conditions. The current study will be followed up with a comprehensive investigation of flare gas reforming and flaring emissions at different physical conditions and fuel mixtures, paving a foundation for further detailed reactive flow computations.

Acknowledgments

The information, data, or work presented herein was funded in part by the Advanced Research Projects Agency-Energy (ARPA-E), U.S. Department of Energy, under Award Number DE-AR0001529, and in part by the National Science Foundation (NSF) under Award Number CBET 2002635. The views and opinions of authors expressed herein do not necessarily state or reflect those of the United States Government or any agency thereof. The authors also acknowledge the Minnesota Supercomputing Institute (MSI) for the computational resources.

References

[1] Brzustowski, T., "Flaring in the energy industry," *Progress in Energy and Combustion Science*, Vol. 2, No. 3, 1976, pp. 129–141.

[2] Fawole, O. G., Cai, X.-M., and MacKenzie, A., "Gas flaring and resultant air pollution: A review focusing on black carbon," *Environmental pollution*, Vol. 216, 2016, pp. 182–197.

[3] Jain, A. K., Briegleb, B. P., Minschwaner, K., and Wuebbles, D. J., "Radiative forcings and global warming potentials of 39 greenhouse gases," *Journal of Geophysical Research: Atmospheres*, Vol. 105, No. D16, 2000, pp. 20773–20790.

[4] Pachauri, R. K., Allen, M. R., Barros, V. R., Broome, J., Cramer, W., Christ, R., Church, J. A., Clarke, L., Dahe, Q., Dasgupta, P., et al., *Climate change 2014: synthesis report. Contribution of Working Groups I, II and III to the fifth assessment report of the Intergovernmental Panel on Climate Change*, Ipcc, 2014.

[5] Ialongo, I., Stepanova, N., Hakkarainen, J., Virta, H., and Gritsenko, D., "Satellite-based estimates of nitrogen oxide and methane emissions from gas flaring and oil production activities in Sakha Republic, Russia," *Atmospheric Environment: X*, Vol. 11, 2021, p. 100114.

[6] Pohl, J., Lee, J., Payne, R., and Tichenor, B., "Combustion efficiency of flares. Report for October 1980-February 1984," Tech. rep., Energy and Environmental Research Corp., Irvine, CA (USA), 1985.

[7] Ismail, O. S., and Umukoro, G. E., "Global impact of gas flaring," 2012.

[8] Kim, W., Mungal, M. G., and Cappelli, M. A., "The role of in situ reforming in plasma enhanced ultra lean premixed methane/air flames," *Combustion and Flame*, Vol. 157, No. 2, 2010, pp. 374–383.

[9] Sun, W., Uddi, M., Won, S. H., Ombrello, T., Carter, C., and Ju, Y., "Kinetic effects of non-equilibrium plasma-assisted methane oxidation on diffusion flame extinction limits," *Combustion and Flame*, Vol. 159, No. 1, 2012, pp. 221–229.

[10] Yang, S., Nagaraja, S., Sun, W., and Yang, V., "Multiscale modeling and general theory of non-equilibrium plasma-assisted ignition and combustion," *Journal of Physics D: Applied Physics*, Vol. 50, No. 43, 2017, p. 433001.

[11] Yang, S., Gao, X., Yang, V., Sun, W., Nagaraja, S., Lefkowitz, J. K., and Ju, Y., "Nanosecond pulsed plasma activated C2H4/O2/Ar mixtures in a flow reactor," *Journal of Propulsion and Power*, Vol. 32, No. 5, 2016, pp. 1240–1252.

[12] Li, X.-S., Zhu, A.-M., Wang, K.-J., Xu, Y., and Song, Z.-M., "Methane conversion to C2 hydrocarbons and hydrogen in atmospheric non-thermal plasmas generated by different electric discharge techniques," *Catalysis Today*, Vol. 98, No. 4, 2004, pp. 617–624.

[13] Johnson, P. N., Taneja, T. S., and Yang, S., "Global Pathway Analysis of Plasma Assisted Ammonia Combustion," *AIAA SCITECH 2022 Forum*, 2022, p. 0977.

[14] Taneja, T. S., and Yang, S., "Numerical Modeling of Plasma Assisted Pyrolysis and Combustion of Ammonia," *AIAA Scitech 2021 Forum*, 2021, p. 1972.

[15] Taneja, T. S., Johnson, P. N., and Yang, S., "Nanosecond pulsed plasma assisted combustion of ammonia-air mixtures: Effects on ignition delays and NOx emission," *Combustion and Flame*, Vol. 245, 2022, p. 112327.

[16] Pancheshnyi, S., Eismann, B., Hagelaar, G., and Pitchford, L., "Computer code zdplaskin," *University of Toulouse, LAPLACE, CNRS-UPS-INP, Toulouse, France*, 2008.

[17] Kee, R. J., Rupley, F. M., Meeks, E., and Miller, J. A., "CHEMKIN-III: A FORTRAN chemical kinetics package for the analysis of gas-phase chemical and plasma kinetics," Tech. rep., Sandia National Lab.(SNL-CA), Livermore, CA (United States), 1996.

[18] Lefkowitz, J. K., Guo, P., Rousso, A., and Ju, Y., "Species and temperature measurements of methane oxidation in a nanosecond repetitively pulsed discharge," *Philosophical Transactions of the Royal Society A: Mathematical, Physical and Engineering Sciences*, Vol. 373, No. 2048, 2015, p. 20140333.

[19] Mao, X., Rousso, A., Chen, Q., and Ju, Y., "Numerical modeling of ignition enhancement of CH4/O2/He mixtures using a hybrid repetitive nanosecond and DC discharge," *Proceedings of the Combustion Institute*, Vol. 37, No. 4, 2019, pp. 5545–5552.

[20] Adamovich, I. V., Nishihara, M., Choi, I., Uddi, M., and Lempert, W. R., "Energy coupling to the plasma in repetitive nanosecond pulse discharges," *Physics of Plasmas*, Vol. 16, No. 11, 2009, p. 113505.

[21] Ju, Y., and Sun, W., "Plasma assisted combustion: Dynamics and chemistry," *Progress in Energy and Combustion Science*, Vol. 48, 2015, pp. 21–83.

[22] Scapinello, M., Delikonstantis, E., and Stefanidis, G. D., "The panorama of plasma-assisted non-oxidative methane reforming," *Chemical Engineering and Processing: Process Intensification*, Vol. 117, 2017, pp. 120–140.

[23] Chen, T. Y., Taneja, T. S., Rousso, A. C., Yang, S., Kolemen, E., and Ju, Y., "Time-resolved in situ measurements and predictions of plasma-assisted methane reforming in a nanosecond-pulsed discharge," *Proceedings of the Combustion Institute*, Vol. 38, No. 4, 2021, pp. 6533–6540.

[24] Pancheshnyi, S., Biagi, S., Bordage, M., Hagelaar, G., Morgan, W., Phelps, A., and Pitchford, L., "The LXCat project: Electron scattering cross sections and swarm parameters for low temperature plasma modeling," *Chemical Physics*, Vol. 398, 2012, pp. 148–153.

[25] "Phelps Database," `www.lxcat.net`, 1987.

[26] "Morgan Database," `www.lxcat.net`, 1987.

[27] "Hayashi Database," `www.lxcat.net`, 1987.

[28] Starikovskiy, A., "Mechanism of plasma-assisted ignition for H2 and C1-C5 hydrocarbons," *55th AIAA Aerospace Sciences Meeting*, 2017, p. 1977.

[29] Zhou, C.-W., Li, Y., Burke, U., Banyon, C., Somers, K. P., Ding, S., Khan, S., Hargis, J. W., Sikes, T., Mathieu, O., et al., "An experimental and chemical kinetic modeling study of 1, 3-butadiene combustion: Ignition delay time and laminar flame speed measurements," *Combustion and Flame*, Vol. 197, 2018, pp. 423–438.

[30] Gao, X., Yang, S., and Sun, W., "A global pathway selection algorithm for the reduction of detailed chemical kinetic mechanisms," *Combustion and Flame*, Vol. 167, 2016, pp. 238–247.

[31] Wang, J., Huang, Z., Tang, C., Miao, H., and Wang, X., "Numerical study of the effect of hydrogen addition on methane–air mixtures combustion," *International journal of hydrogen energy*, Vol. 34, No. 2, 2009, pp. 1084–1096.

[32] Zhong, B.-J., and Peng, H.-S., "Experimental and kinetic investigations of the effect of H2/CH4/C2H4 addition on the burning properties of practical jet fuel," *Proceedings of the Combustion Institute*, Vol. 37, No. 2, 2019, pp. 1673–1681.

[33] Ju, Y., Lefkowitz, J. K., Reuter, C. B., Won, S. H., Yang, X., Yang, S., Sun, W., Jiang, Z., and Chen, Q., "Plasma assisted low temperature combustion," *Plasma Chemistry and Plasma Processing*, Vol. 36, No. 1, 2016, pp. 85–105.